

Superconductivity in single crystalline Pb nanowires contacted by normal metal electrodesJian Wang,^{1,2,*} Yi Sun,^{1,†} Mingliang Tian,^{2,3} Bangzhi Liu,⁴ Meenakshi Singh,² and Moses H. W. Chan^{2,‡}¹*International Center for Quantum Materials, School of Physics, Peking University, Beijing 100871, People's Republic of China*²*Center for Nanoscale Science and Department of Physics, Pennsylvania State University, University Park, Pennsylvania 16802-6300, USA*³*High Magnetic Field Laboratory, Chinese Academy of Science, Hefei 230031, Anhui, People's Republic of China*⁴*Materials Research Institute, Pennsylvania State University, University Park, Pennsylvania 16802-6300, USA*

(Received 29 January 2012; published 24 July 2012)

The transport properties of superconducting single crystal Pb nanowires that are 55 and 70 nm in diameter were studied by the standard four-electrode method. With normal metal electrodes, resistance-temperature and resistance-magnetic field scans show a series of resistance steps with increasing temperature and magnetic field as the wires are brought toward the normal state. The resistance-current (R - I) scans at different temperatures and magnetic fields show that the increase in R with I is punctuated with sharp steps at specific current values. A large residual resistance is observed down to 2 K. The origin of these phenomena is related to the inhomogeneity and proximity effect from the normal electrodes.

DOI: 10.1103/PhysRevB.86.035439

PACS number(s): 74.25.F-, 74.45.+c, 74.78.Na, 73.63.-b

I. INTRODUCTION

The study of superconductivity in nanowires and quasi-one-dimensional nanostructures is driven both by open questions in these systems and by their potential applications in dissipationless electronic devices.¹⁻¹⁶ Low-dimensional Pb nanostructures have been extensively studied for decades.^{5-12, 16-18} In addition, amorphous and granular nanowires of Pb and other superconducting materials have been studied.^{1, 17-21} In the last few years, a number of experiments have studied the properties of single crystal superconducting nanowires with a diameter of less than 100 nm.^{13, 14, 22-24} An overarching theme of these studies is to understand how superconductivity in these wires is suppressed with decreasing diameter. It has been generally accepted that when the diameter of the nanowires is reduced toward and below the Ginzburg-Landau phase coherence length and the magnetic penetration depth,²⁵ the superconductivity is suppressed via thermally activated phase slip²⁶⁻²⁸ and quantum phase slip processes.^{2, 3, 29, 30}

The transport properties of a superconducting nanowire (and indeed any nanowire) are expected to be strongly influenced by the electrodes contacting the wire. The electrode effect on crystalline nanowires has recently been systematically studied. When contacted by superconducting electrodes, normal (Au)⁵ and magnetic (Co and Ni)³¹ nanowires acquire superconductivity via the proximity effect. A counterintuitive phenomenon known as the antiproximity was also observed, where the superconductivity of thin Zn and Al nanowires was suppressed or weakened when they were contacted by superconducting electrodes.^{14, 23, 32} Surprisingly, the effect of normal electrodes on single crystal superconducting nanowires has not been systematically studied by standard four-probe transport measurements.

In this paper, we report on such a study of individual single crystal superconducting Pb nanowires of 55 and 70 nm in diameter contacted by four normal Pt electrodes. The diameters of these wires are on the order of the coherence lengths of Pb. Interestingly, resistance-temperature (R - T), resistance-magnetic field (R - H), and resistance-current (R - I) scans all show a series of resistance steps with increasing temperature, magnetic field, and excitation current, respectively, as

the wires are brought toward the normal state. A large residual resistance is also observed. We attribute these observations to the weakening of superconductivity in the Pb nanowires by the normal Pt electrodes.

II. RESULTS AND DISCUSSION

The Pb nanowires used in this work were electrodeposited in commercially available track-etched porous polycarbonate membranes that are coated with Au on one side.¹³ The electrolyte $\text{Pb}(\text{NH}_2\text{SO}_3)_2$ was prepared by reacting lead carbonate (PbCO_3) with excess sulfamic acid solution in purified H_2O (resistivity $> 18\text{M } \Omega \text{ cm}$). The transmission electron microscopy (TEM) and selected area electron diffraction study showed that the Pb nanowires were single crystalline (Fig. 1). A 3- to 4-nm-thick oxide shell surrounding the nanowires was observed, which plays a role in protecting the nanowires from getting damaged during the attachment of the electrodes. Electrical contact to an individual Pb nanowire was made by the following procedure. A drop of the nanowire suspension solution is placed on a silicon substrate with a 1- μm -thick Si_3N_4 insulating layer. The sample is then transferred into a focused ion beam (FIB) etching and deposition system (FEI Quanta 200 3D). Four FIB-assisted Pt strips are deposited onto and make ohmic contact to the Pb nanowire. The deposition current is set to be less than 10 pA to minimize any damage to the nanowire. A scanning electron micrograph (SEM) of the 55-nm Pb wire contacted in this manner is shown in the inset of Fig. 2(a). Transport measurements are carried out in a physical property measurement system cryostat (Quantum Design).

Figure 2 shows the temperature dependence of the electronic transport for the 55- and 70-nm-diameter nanowires. The distances between two inner edges of the two voltage (V) electrodes of the 70- and 55-nm samples were 1.9 and 3.7 μm , respectively. Figure 2(a) shows the R - T curve of a 55-nm wire measured with an excitation current of 50 nA from 1.8 to 300 K at zero magnetic field. The temperature dependence of the resistivities (ρ) of the two wires near and below the superconducting transition temperature (T_C) of Pb at different magnetic fields are shown more clearly

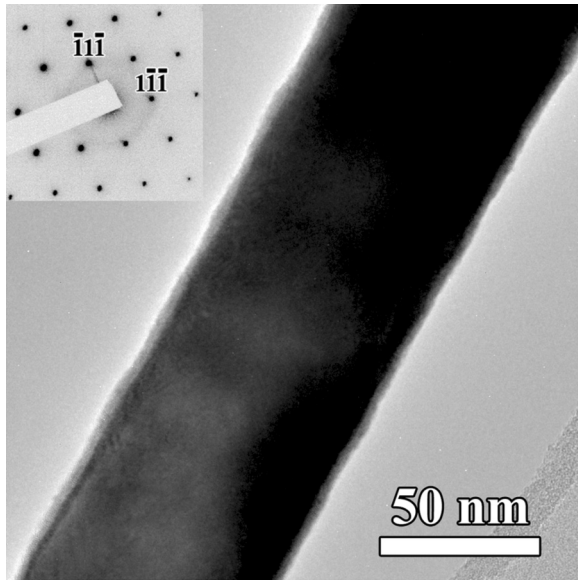


FIG. 1. TEM image of a typical Pb nanowire. The inset shows the [110] zone pattern from the same wire.

in Figs. 2(b) and 2(c). The excitation current employed in these measurements is 500 nA. The magnetic field was aligned perpendicular to the nanowires. Two obvious resistance drops at 7.0 and 4.9 K are seen in the R - T dependence of the 55-nm wire [Fig. 2(b)]. For the first step, the resistance decreases by 14% of the normal state value between 6.5 and 7.0 K. The resistance drop at the second step at 4.9 K is more gradual. Both steps move to low temperature with increasing field. The wire is normal at an applied field of 20 kOe at 2 K. The ρ - T curves of 70-nm nanowire [Fig. 2(c)] show three steps at 6.98, 5.90, and 4.67 K. It is reasonable to attribute the resistance drops near 7.0 K found for both wires to the “intrinsic” superconducting transition of the Pb nanowires, because the T_C of bulk Pb is 7.2 K. What, then, is the origin of the resistance steps well below T_C ? According to the TEM images, the nanowire is single crystal and homogeneous. But when the Pt electrodes are deposited onto the nanowires, the FIB fabrication process may introduce inhomogeneity in the contact region. For example, the wire in the contact region may become thinner and contaminated by Ga atoms. The characteristic range of the inhomogeneity region is found to be on the order of ~ 190 nm in our samples.³⁵ This number is reasonable given that the width of the Pt electrodes is on the scale of ~ 190 nm.

Regular resistance steps in R vs T curves were reported in microscale Sn whiskers ($1 \mu\text{m} \times 1 \mu\text{m} \times 1 \text{mm}$) contacted with multiple normal Cu electrodes spaced out along the whisker with the distance between neighboring electrodes ranging from 1.5 to $10.5 \mu\text{m}$.³⁴ By making measurements across different electrodes, the authors were able to identify each resistance step as the superconducting transition of a specific section of the whisker. They found the average domain length contributing to each step to be 20–900 nm. The observed steps are attributed to the effect of the normal metal electrodes on the superconductor.³⁴ The resistance steps found here at temperatures well below 7 K may have the same origin as that found in Ref. 34. However, in our situation, a finite resistance

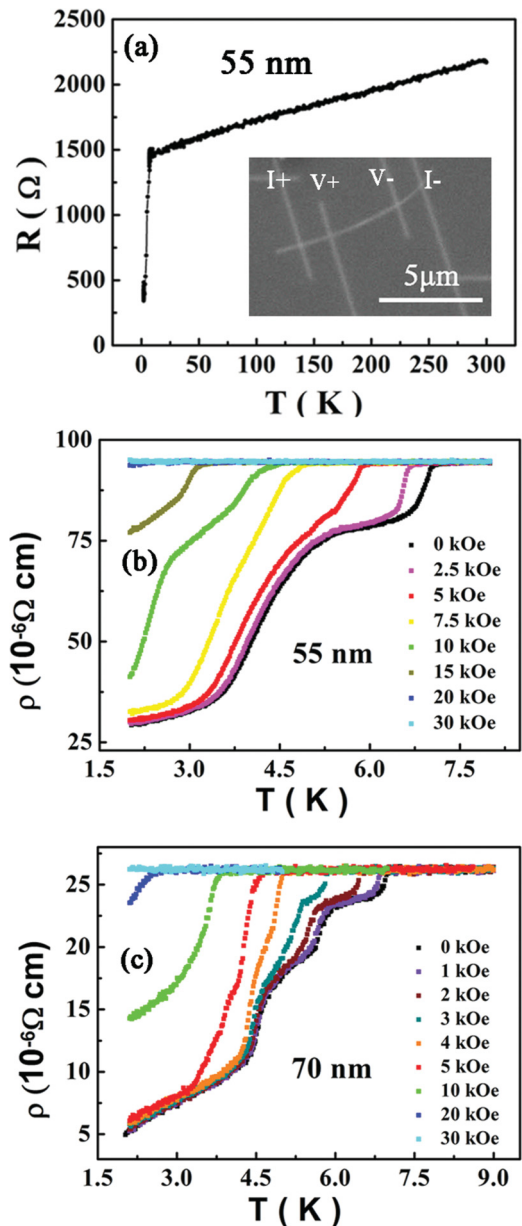


FIG. 2. (Color online) (a) Resistance vs temperature of 55-nm Pb nanowires in the wide temperature range. Inset is the SEM image of the four-electrode measurement. (b) and (c) Resistivity vs temperature of 55- and 70-nm Pb nanowires near and below the T_C in different magnetic fields.

of 20% and 30% of the normal state resistance is found down to 2 K. This is unlikely to be due to the inhomogeneity in the wire, because the inhomogeneity extends only ~ 190 nm out of a total length of 1.9 and $3.7 \mu\text{m}$.

The normal Pt electrodes are expected to have a “reversed” proximity effect on the superconducting Pb nanowires. This effect weakens the superconductivity of the Pb nanowires and may account for the residual resistance at temperatures well below T_C of Pb. If the residual resistance is indeed due to this “reversed” proximity effect, the range of this effect can be estimated to be ~ 180 and ~ 550 nm for the 70- and 55-nm nanowires, respectively. This range is consistent with the range of the regular proximity effect induced by superconducting

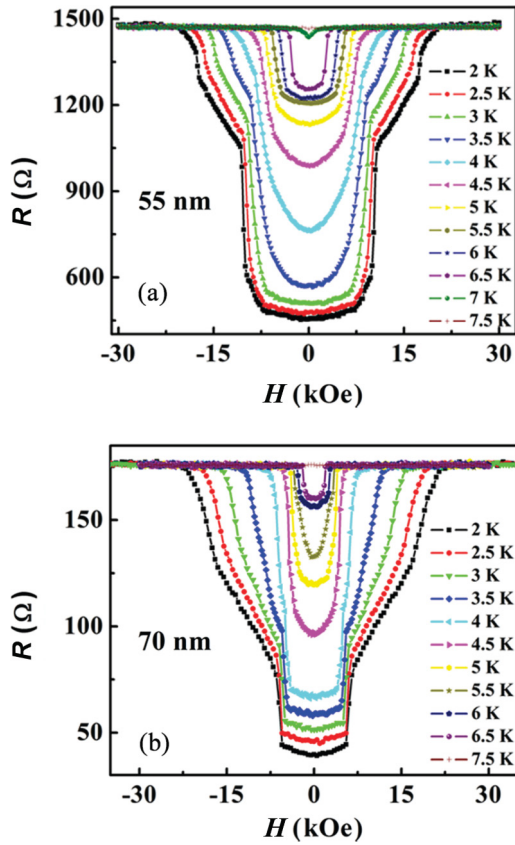


FIG. 3. (Color online) Resistance vs magnetic field of 55- and 70-nm Pb nanowires at different temperatures.

electrodes on a normal nanowire.⁵ The resistivities of the 70- and 55-nm Pb nanowires at room temperature are 26×10^{-6}

and $94 \times 10^{-6} \Omega \text{ cm}$, respectively. These numbers are on the same order as the resistivity of bulk Pb ($21.3 \times 10^{-6} \Omega \text{ cm}$). The larger ρ of the thinner wire is probably the effect of enhanced surface scattering. In our four-probe measurement configuration, the contact resistance can be neglected.

Figure 3 shows the resistance of the Pb nanowires as a function of the magnetic field perpendicular to the nanowires at different temperatures. The excitation current is 500 nA for the 55-nm wire and 1 μA for the 70-nm wire. Sharp and well-defined resistance steps are found in R vs H scans at low temperature [Figs. 3(a) and 3(b)]. The first step was found near 10 kOe for the 55-nm wire and 7.2 kOe for the 70-nm wire. The magnitudes of the resistance steps in the R - H scans at different temperatures are consistent with the steps found in the R - T scans at different field values. Substantial residual resistances near zero field at low temperature are clearly displayed. The fields at which the two wires are driven into the normal state are almost same (21 kOe) but much larger than that of the bulk Pb (0.803 kOe at zero temperature and 0.74 kOe at 2.0 K). This enhancement in the critical field is a well-studied phenomenon in nanoscale superconductors.³⁵ With increasing temperature, the critical field decreases and the steps become less well defined and rounded.

The R - I curves of the two Pb nanowires measured at different temperatures under zero field are shown in Figs. 4(a) and 4(c); the measurements under different perpendicular magnetic fields at 2 K are shown in Figs. 4(b) and 4(d). The corresponding V - I scans at zero field at different temperatures and the V - I scans at different fields at 2 K of the 70-nm wire are shown in Figs. 4(e) and 4(f), respectively. Similar dependences on the excitation current are found in the two wires. The increase in R and V with increasing I is punctuated

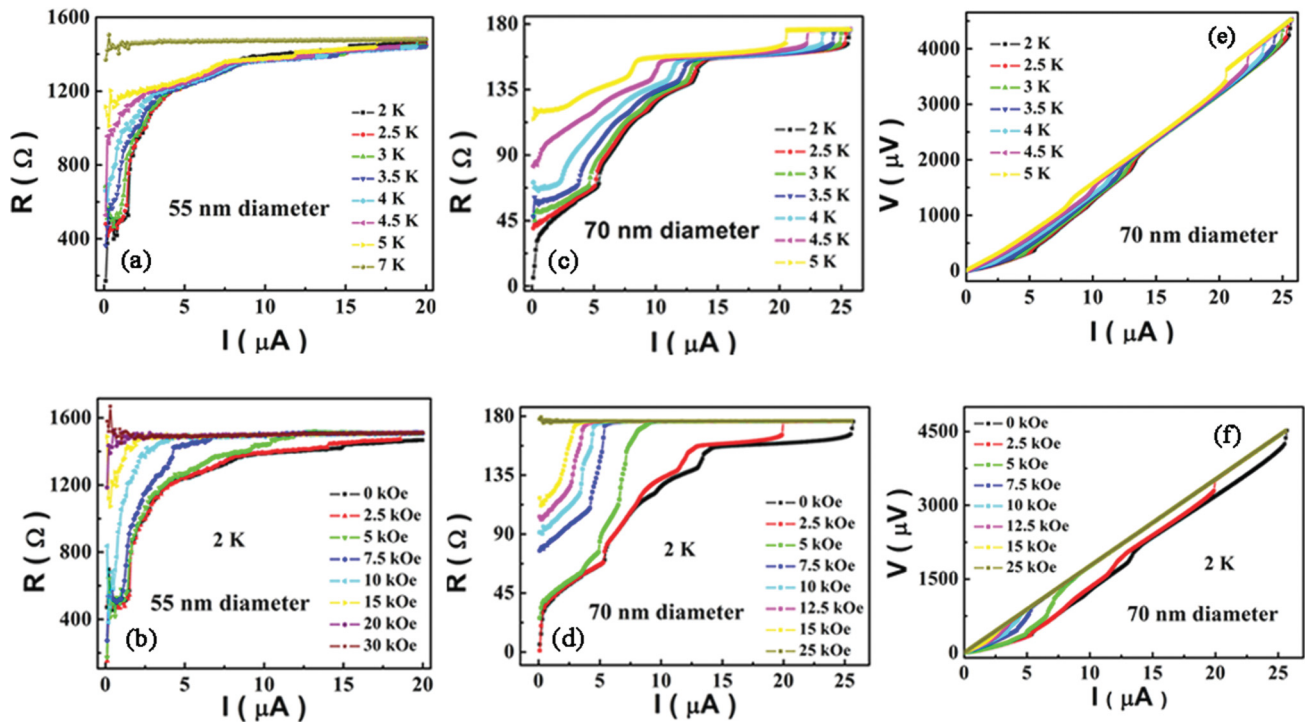


FIG. 4. (Color online) Resistance vs current of 55- and 70-nm Pb nanowires (a) and (c) at different temperatures and (b) and (d) in different magnetic fields. Voltage vs current curves of 70-nm Pb nanowires (e) at different temperatures and (f) in different magnetic fields.

by sharp steps. Figure 4(d) shows that the resistance of 70-nm wire at 2 K reaches almost zero in the low current limit of our measurement at 50 nA, but the 55-nm sample [in Fig. 4(b)] shows a residual resistance of $\sim 10^2 \Omega$. Unfortunately, we were limited by our equipment and measurement noise from extending the measurement to lower current and temperature. The normal state resistance of 180Ω of the 70-nm wire at 2 K and zero field is reached with stepwise increase in resistance at 50 nA and 5.40, 9.47, 13.00, and $25.47 \mu\text{A}$. At higher temperatures, the first step is no longer found and the other steps move to lower current values. Under a field of 2.5 kOe at 2 K, the resistance steps also move to lower current values [Fig. 4(d)]. Similar dependence of these “critical” current-like resistance steps on temperature and magnetic field have been reported in superconducting whiskers,^{35,37} microbridges,³⁸ and nanowires.^{13,23,39–41} The observed V - I steps are reminiscent of phase slip center (PSC) behavior. However, there are some differences between the conventional PSCs and our observations. In experiments that display standard PSC behavior, a true zero resistance state is found below a certain threshold bias current. With increasing current, the resistance increases with uniform steps above this threshold current. In our situation, the resistance steps are not uniform, and in the case of the 55-nm wire, a large residual resistance is found even at the lowest excitation current. The residual resistance, as explained earlier, is a consequence of the “reverse” proximity effect. The nonuniformity of the steps might be a consequence of the inhomogeneity introduced in the Pb wires during FIB-assisted deposition of the Pt electrodes.

The inhomogeneity introduced by the electrodes may not have played an important role in the earlier studies of PSCs, because the length of the wires was relatively long or the electrode deposition process was less invasive.

III. CONCLUSIONS

Single crystal Pb nanowires of two diameters were fabricated by electrochemical deposition. R - T , R - H , and R - I curves measured by a standard four-probe configuration showed a series of resistance steps with increasing temperature, magnetic field, and excitation current, respectively. Residual resistances were also observed under T_C . We attribute these phenomena to the inhomogeneity and proximity effect introduced by the normal metal (Pt) electrodes.

ACKNOWLEDGMENTS

This work was financially supported by the Pennsylvania State University Materials Research Science and Engineering Center under National Science Foundation Grant No. DMR-0820404, the National Basic Research Program of China (Grant No. 2012CB921300), the National Natural Science Foundation of China (Grant No. 11174007), National Key Basic Research of China (under Grant No. 2011CBA00111), the National Natural Science Foundation of China (Grant No. 11174294), and the China Postdoctoral Science Foundation (Grant No. 2011M500180).

*jianwangphysics@pku.edu.cn

[†]yisun@pku.edu.cn

[‡]chan@phys.psu.edu

¹A. Bezryadin, C. N. Lau, and M. Tinkham, *Nature (London)* **404**, 971 (2000).

²K. Y. Arutyunov, D. S. Golubev, and A. D. Zaikin, *Phys. Rep.* **464**, 1 (2008).

³D. S. Golubev and A. D. Zaikin, *Phys. Rev. B* **64**, 014504 (2001).

⁴N. Giordano, *Phys. Rev. Lett.* **61**, 2137 (1988).

⁵J. Wang, C. T. Shi, M. Tian, Q. Zhang, N. Kumar, J. K. Jain, T. E. Mallouk, and M. H. W. Chan, *Phys. Rev. Lett.* **102**, 247003 (2009).

⁶J. Wang, X. C. Ma, L. Lu, A. Z. Jin, C. Z. Gu, X. C. Xie, J. F. Jia, X. Chen, and Q. K. Xue, *Appl. Phys. Lett.* **92**, 233119 (2008).

⁷J. Wang, X. C. Ma, Y. Qi, Y. S. Fu, S. H. Ji, L. Lu, J. F. Jia, and Q. K. Xue, *Appl. Phys. Lett.* **90**, 113109 (2007).

⁸J. Wang, X. C. Ma, Y. Qi, Y. S. Fu, S. H. Ji, L. Lu, A. Z. Jin, C. Z. Gu, X. C. Xie, M. Tian, J. F. Jia, and Q. K. Xue, *J. Appl. Phys.* **106**, 034301 (2009).

⁹J. Wang, J. F. Jia, X. C. Ma, Q. T. Shen, T. Z. Han, A. Z. Jin, L. Lu, C. Z. Gu, M. Tian, X. C. Xie, X. Chen, and Q. K. Xue, *J. Vac. Sci. Technol. B* **28**, 678 (2010).

¹⁰J. Wang, X. C. Ma, S. H. Ji, Y. Qi, Y. S. Fu, A. Z. Jin, L. Lu, C. Z. Gu, X. C. Xie, M. Tian, J. F. Jia, and Q. K. Xue, *Nano Res.* **2**, 671 (2009).

¹¹J. Wang, X. C. Ma, Y. Qi, Y. S. Fu, S. H. Ji, L. Lu, X. C. Xie, J. F. Jia, X. Chen, and Q. K. Xue, *Nanotechnology* **19**, 475708 (2008).

¹²Z. L. Guan, Y. X. Ning, C. L. Song, J. Wang, J. F. Jia, X. Chen, Q. K. Xue, and X. Ma, *Phys. Rev. B* **81**, 054516 (2010).

¹³M. Tian, J. Wang, J. S. Kurtz, Y. Liu, M. H. W. Chan, T. S. Mayer, and T. E. Mallouk, *Phys. Rev. B* **71**, 104521 (2005).

¹⁴M. Tian, N. Kumar, S. Y. Xu, J. Wang, J. S. Kurtz, and M. H. W. Chan, *Phys. Rev. Lett.* **95**, 076802 (2005).

¹⁵J. Hua, Z. L. Xiao, A. Imre, S. H. Yu, U. Patel, L. E. Ocola, R. Divan, A. Koshelev, J. Pearson, U. Welp, and W. K. Kwok, *Phys. Rev. Lett.* **101**, 077003 (2008).

¹⁶Y. Guo, Y. F. Zhang, X. Y. Bao, T. Z. Han, Z. Tang, L. X. Zhang, W. G. Zhu, E. G. Wang, Q. Niu, Z. Q. Qiu, J. F. Jia, Z. X. Zhao, and Q. K. Xue, *Science* **306**, 1915 (2004).

¹⁷P. Xiong, A. V. Herzog, and R. C. Dynes, *Phys. Rev. Lett.* **78**, 927 (1997).

¹⁸A. V. Herzog, P. Xiong, F. Sharifi, and R. C. Dynes, *Phys. Rev. Lett.* **76**, 668 (1996).

¹⁹S. Michotte, S. Mátéfi-Tempfli, and L. Piroux, *Appl. Phys. Lett.* **82**, 4119 (2003).

²⁰S. Michotte, S. Mátéfi-Tempfli, and L. Piroux, *Supercond. Sci. Technol.* **16**, 557 (2003).

²¹F. Altomare, A. M. Chang, M. R. Melloch, Y. G. Hong, and C. W. Tu, *Phys. Rev. Lett.* **97**, 017001 (2006).

²²M. Tian, J. Wang, N. Kumar, T. H. Han, Y. Kobayashi, Y. Liu, T. E. Mallouk, and M. H. W. Chan, *Nano Lett.* **6**, 2773 (2006).

- ²³M. Tian, N. Kumar, J. Wang, S. Y. Xu, and M. H. W. Chan, *Phys. Rev. B* **74**, 014515 (2006).
- ²⁴H. D. Liu, Z. X. Ye, Z. P. Luo, K. D. D. Rathnayaka, and W. H. Wu, *Phys. C* **468**, 304 (2008).
- ²⁵W. J. Skocpol and M. Tinkham, *Rep. Prog. Phys.* **38**, 1049 (1975).
- ²⁶W. A. Little, *Phys. Rev.* **156**, 396 (1967).
- ²⁷J. S. Langer and V. Ambegaokar, *Phys. Rev.* **164**, 498 (1967).
- ²⁸D. E. McCumber and B. I. Halperin, *Phys. Rev. B* **1**, 1054 (1970).
- ²⁹A. D. Zaikin, D. S. Golubev, A. van Otterlo, and G. T. Zimanyi, *Phys. Rev. Lett.* **78**, 1552 (1997).
- ³⁰J. M. Duan, *Phys. Rev. Lett.* **74**, 5128 (1995).
- ³¹J. Wang, M. Singh, M. Tian, N. Kumar, B. Z. Liu, C. T. Shi, J. K. Jain, N. Samarth, T. E. Mallouk, and M. H. W. Chan, *Nat. Phys.* **6**, 389 (2010).
- ³²M. Singh, J. Wang, M. Tian, T. E. Mallouk, and M. H. W. Chan, *Phys. Rev. B* **83**, 220506 (2011).
- ³³K. Y. Arutyunov, D. A. Presnov, S. V. Lotkhov, A. B. Pavolotski, and L. Rinderer, *Phys. Rev. B* **59**, 6487 (1999).
- ³⁴K. Y. Arutyunov, T. V. Ryyänen, J. P. Pekola, and A. B. Pavolotski, *Phys. Rev. B* **63**, 092506 (2001).
- ³⁵S. Dubois, A. Michel, J. P. Eymery, J. L. Duvail, and L. Piraux, *J. Mater. Res.* **14**, 665 (1999).
- ³⁶J. Meyer and G. V. Minniger, *Phys. Lett.* **38**, 529 (1972).
- ³⁷U. Schulz and R. Tidecks, *Solid State Comm.* **57**, 829 (1986).
- ³⁸W. J. Skocpol, M. R. Beasley, and M. Tinkham, *J. Low Temp. Phys.* **16**, 145 (1974).
- ³⁹D. Y. Vodolazov, F. M. Peeters, L. Piraux, S. Mátéfi-Tempfli, and S. Michotte, *Phys. Rev. Lett.* **91**, 157001 (2003).
- ⁴⁰D. Lucot, F. Pierre, D. Mailly, K. Yu-Zhang, S. Michotte, F. de Menten de Horne, and L. Piraux, *Appl. Phys. Lett.* **91**, 042502 (2007).
- ⁴¹H. D. Liu, Z. X. Ye, W. H. Wu, and K. D. D. Rathnayaka, *J. Appl. Phys.* **105**, 07E305 (2009).